Interplay of Aspect Ratio and Emission Dipole Orientation for Light Extraction in Corrugated Red, Green and Blue OLEDs

Milan Kovačič *, Janez Krč and Marko Topič *

Laboratory of Photovoltaics and Optoelectronics, Faculty of Electrical Engineering, University of Ljubljana, 1000 Ljubljana, Slovenia; janez.krc@fe.uni-lj.si
* Correspondence: MK: milan.kovacic@fe.uni-lj.si, MT: marko.topic@fe.uni-lj.si

Supplementary figures

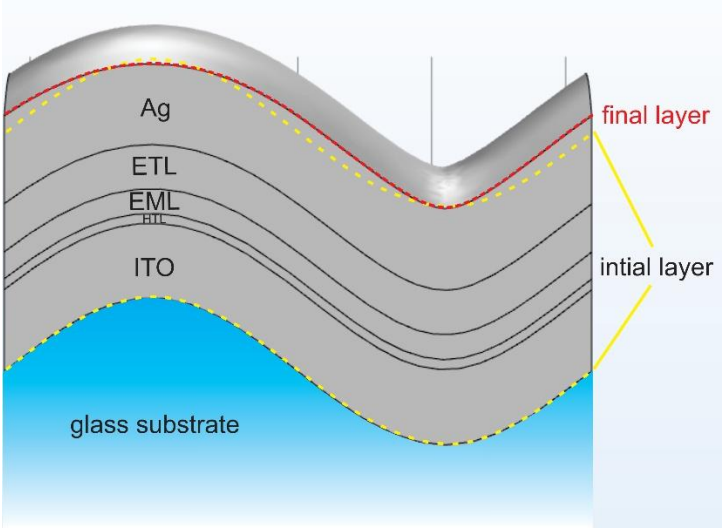


Figure S1. Cross-sectional view of layer growth on a regular 2D sine-shaped texture (P = 800 nm, h = 400 nm). Shown is the stack configuration for a blue OLED, with layer thicknesses of 90, 12, 30, 54, and 100 nm. The figure highlights the transition from the original sine-shaped surface (yellow line) to the altered final layer profile (red line).

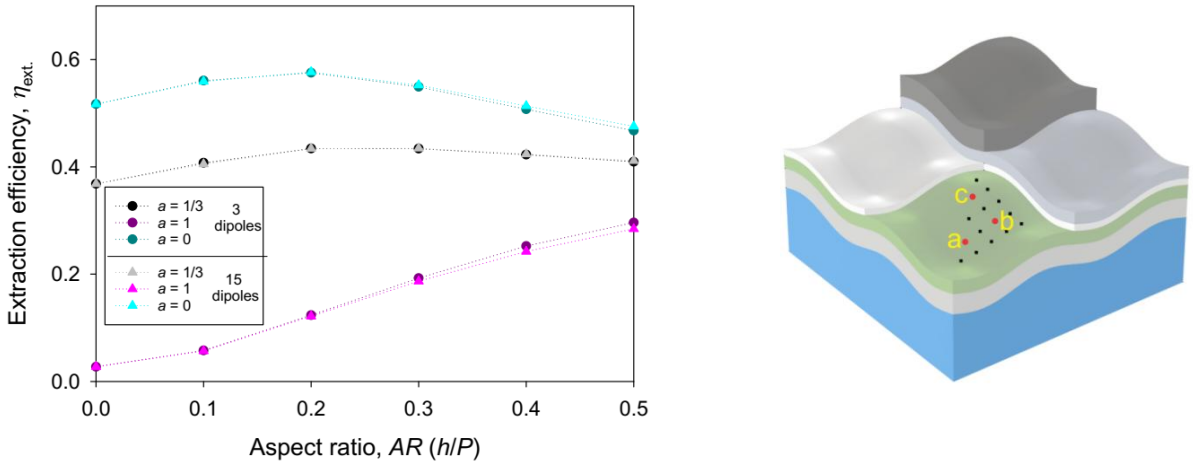


Figure S2. a) Light extraction, for blue OLED with P = 800 nm and different heights, for the case with 3 or 15 selected dipoles and 3 preferential dipole orientations. b) Representation of 3 selected dipole positions (a, b, c) and a collection of 15 dipoles.

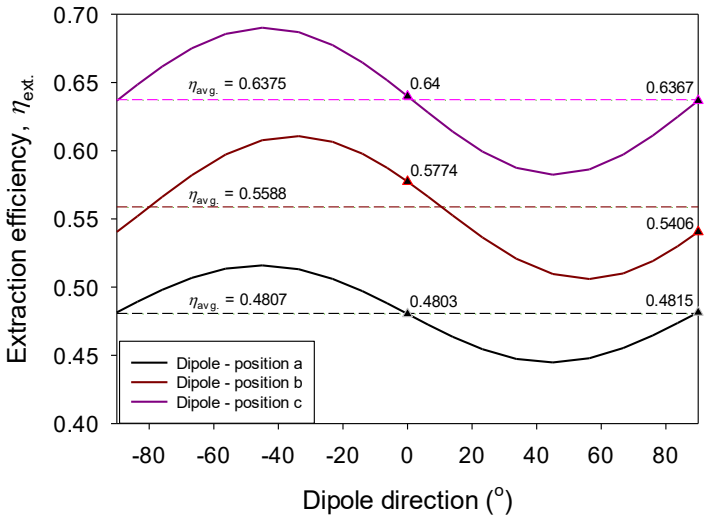
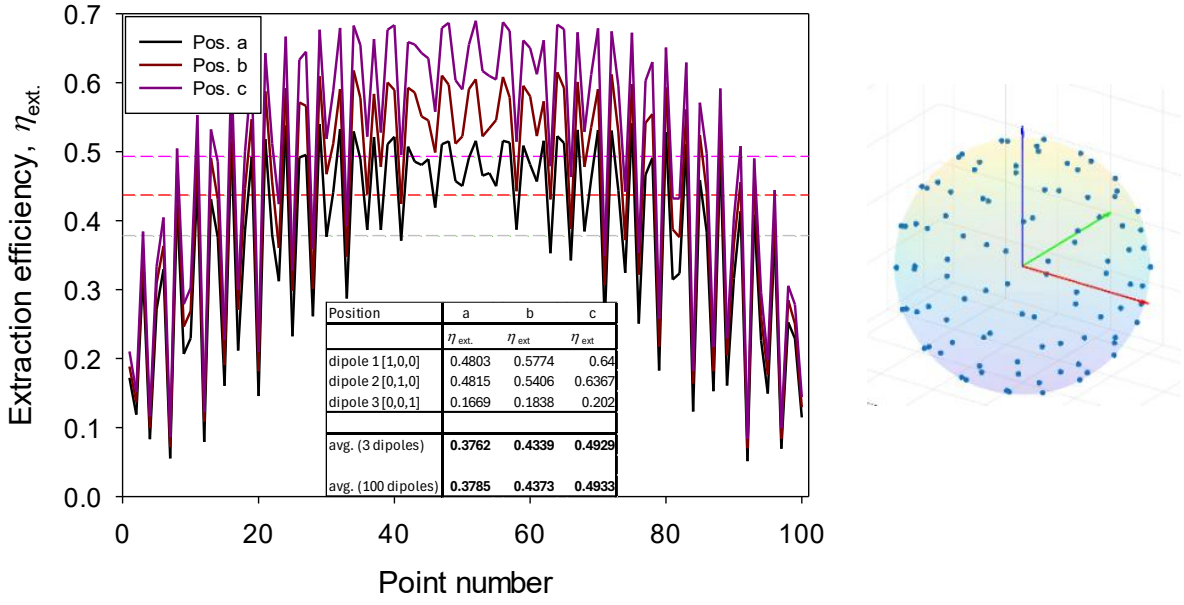


Figure S3. Light extraction (blue OLED with P = 800 nm, h = 240 nm and λ = 460 nm) for horizontally oriented dipoles on a corrugated structure, evaluated at three discrete positions (a, b, c – see **Figure S2b**) as used in the simulations. The dashed lines show the in-plane orientation average corresponding to a random (azimuthally uniform) horizontal distribution; this average is accurately captured by the mean of two orthogonal horizontal dipoles (values marked with triangular symbols).



Position	a	b	c
	$\eta_{ext.}$	η_{ext}	η_{ext}
dipole 1 [1,0,0]	0.4803	0.5774	0.64
dipole 2 [0,1,0]	0.4815	0.5406	0.6367
dipole 3 [0,0,1]	0.1669	0.1838	0.202
avg. (3 dipoles)	**0.3762**	**0.4339**	**0.4929**
avg. (100 dipoles)	**0.3785**	**0.4373**	**0.4933**

a) **b)**

Figure S4. a) Extraction efficiency (blue OLED with P = 800 nm, h = 240 nm and λ = 460 nm) for multiple emitter orientations (each orientation is presented by one of 100 dipole directions presented on the right side), shown for three discrete texture positions (a, b, c– see **Figure S2b**). The dashed lines denote the orientation-averaged response computed from all 100 orientations or from three orthogonal dipoles, demonstrating that the reduced-basis averaging accurately represents the ensemble and validating our approach. The actual data are provided in the inset. b) Illustration of a uniform (isotropic) distribution of dipole orientations (100 points), corresponding to random orientation across multiple periods. Simulations show that the orientation-averaged response is accurately reproduced by averaging over three orthogonal basis dipoles (red, green and blue arrows in the figure). Same set of basis dipoles was used in our simulations.

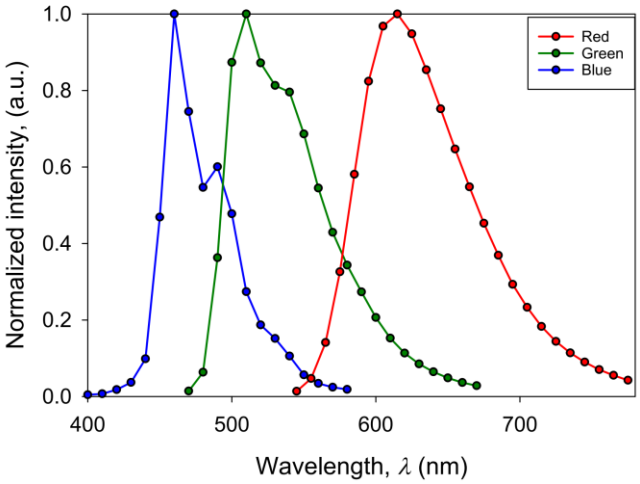


Figure S5. Emission spectra of used materials

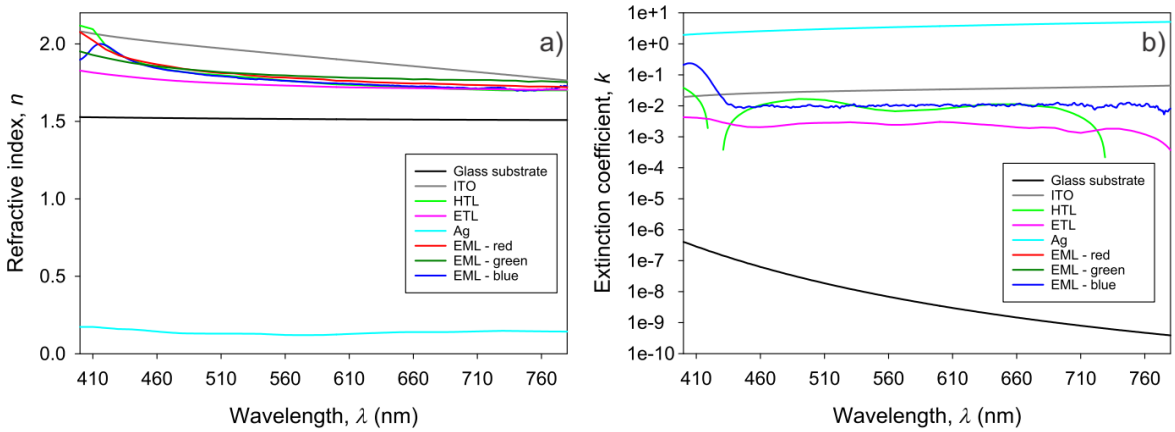


Figure S6. Complex refractive indices of used materials. a) Refractive indices, b) Extinction coefficient

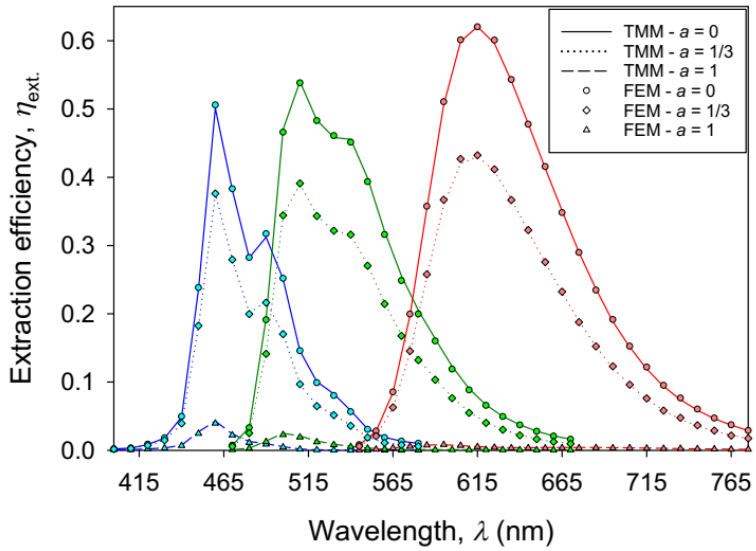


Figure S7. Validation of the FEM implementation by comparison with the exact TMM for planar stacks (red, green and blue device). TMM has been repeatedly verified against experimental data. No separate external benchmark was performed for the corrugated case; however, the same physical assumptions, boundary conditions, and material models apply, and prior work (Zschiedrich, L. et. all - Ref. [50,51]) establishes the suitability of FEM for periodically textured optical structures.

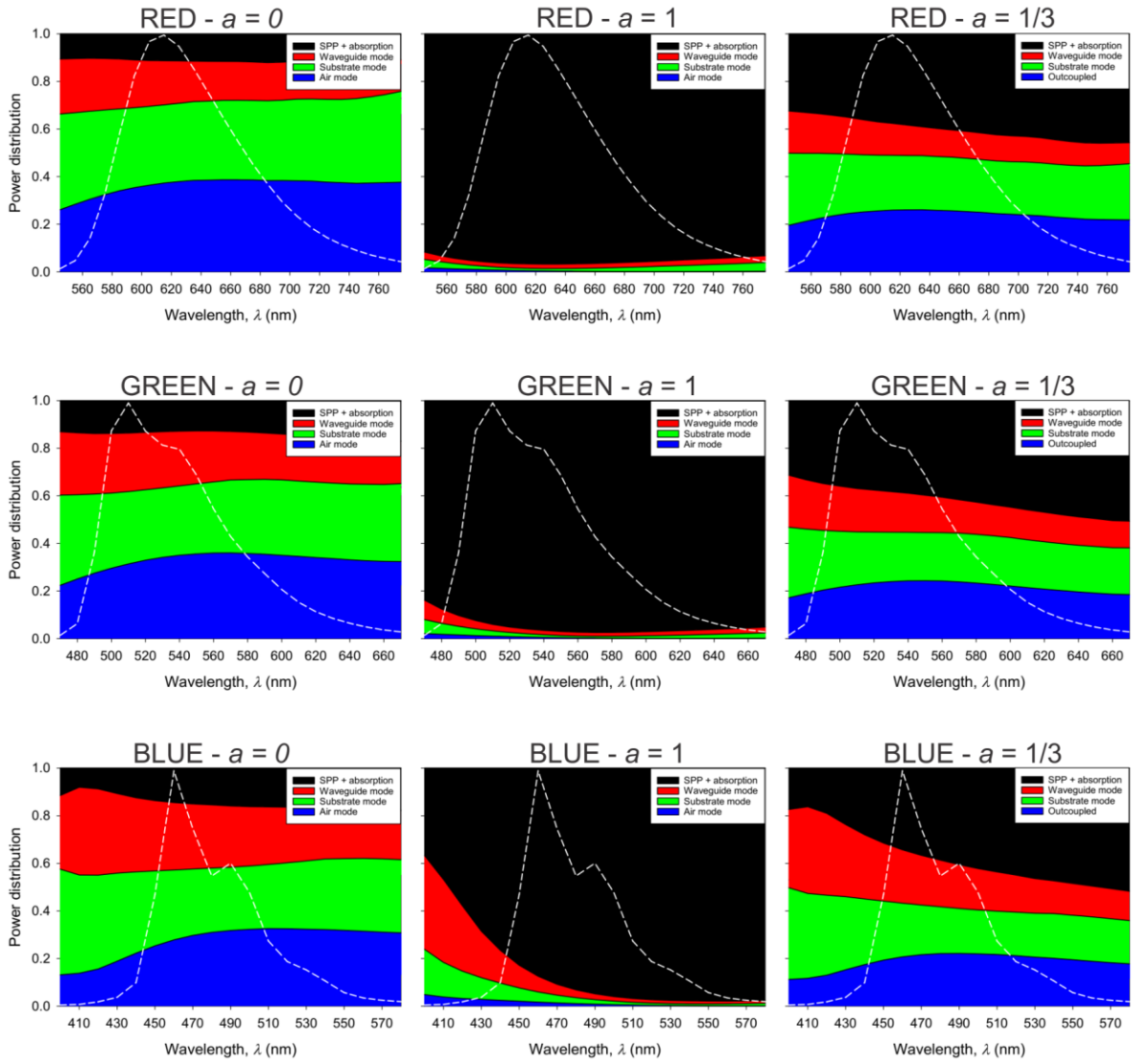


Figure S8. Power mode analysis of flat devices separated for different anisotropy values

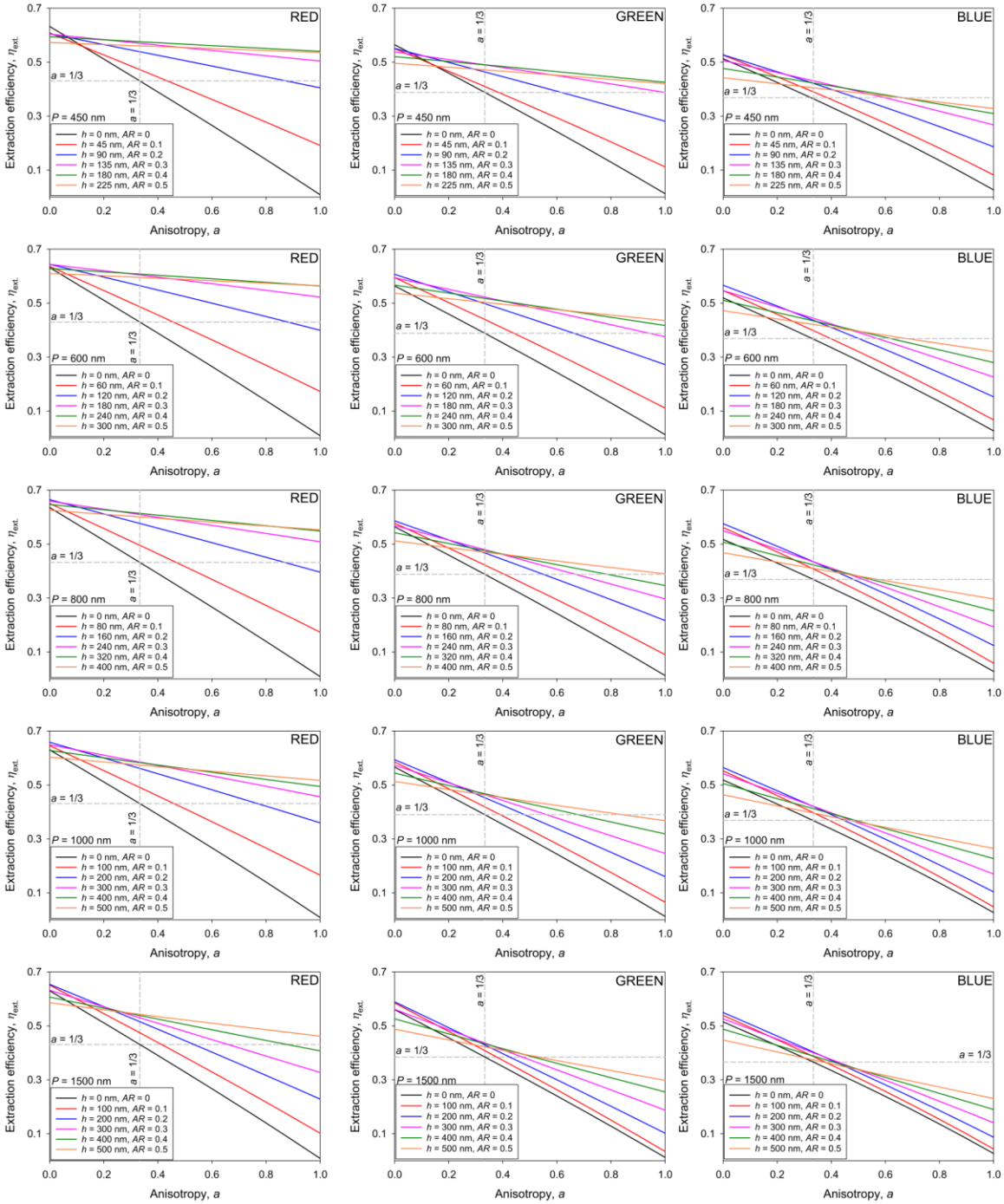


Figure S9. Light extraction regarding to initial anisotropy values for different periods of corrugation.

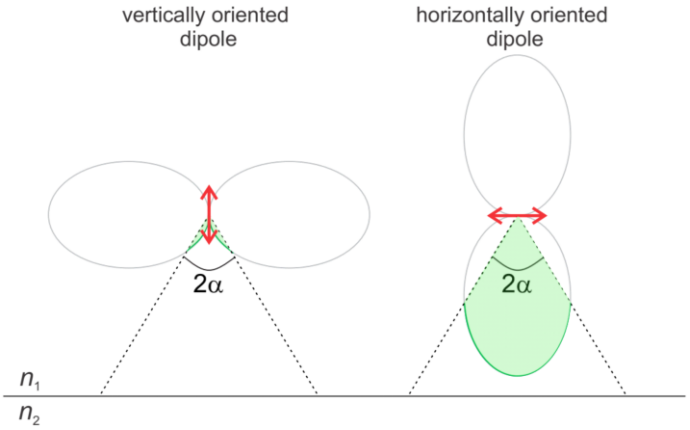


Figure S10. Angular intensity distribution of horizontally and vertically oriented dipoles, with illustration of escape cones (2α) according to interface between two materials.